Determination of Supercooled Liquid Water Content by Measuring Rime Rate

DAVID C. ROGERS, DARREL BAUMGARDNER[1] AND GABOR VALI

Department of Atmospheric Science, University of Wyoming, Laramie 82071

(Manuscript received 23 December 1981, in final form 26 August 1982)

ABSTRACT

A ground-based technique is described for determining the liquid water content of supercooled clouds or fog by measuring the mass rate of rime accumulation on a small rotating wire. Development of the technique is described, examples of the data are presented, and comparisons are made with two conventional methods of liquid water measurement. The comparisons were quite favorable for the winter orographic clouds studied.

1. Introduction

Cloud liquid water content (LWC) has usually been measured from aircraft with a variety of approaches including such diverse techniques as measuring the latent heat needed to evaporate cloud water intercepted by a heated wire (e.g., King *et al.*, 1978), measuring the resistance across paper wetted by cloud water (Warner and Newnham, 1952), impaction and imprint devices (Squires and Gillespie, 1952), long path length optical attenuation at infrared wavelengths through the cloud (Chylek, 1978), short path length optical attenuation at visible wavelengths through the ambient vapor and evaporated cloud (Kyle, 1975), and optical scattering from individual droplets (summarized in Dytch and Carrera, 1976). The development of many of the earlier techniques was prompted by aircraft icing studies in supercooled water clouds, and so various types of rime ice mass or depth instruments have also been devised, including a rotating disc and a rotating multicylinder (Brun *et al.*, 1955). Recently, a transverse vibrating wire has been used as part of a radiosonde package for measuring supercooled LWC (Hill and Woffinden, 1980). For techniques which rely on first collecting the water and then measuring, cold cloud conditions offer different problems than warm clouds because the character of the water deposit depends on the temperature of the cloud and of the collector surface, the droplet size distribution and the relative speed of the cloud and collector (Macklin, 1962).

The technique described here differs from the others mentioned in that the measurements are made at a stationary location at the earth's surface in supercooled fog or surface based clouds. The relative airspeed of cloud and collector is obtained by rotating a collecting wire fast enough that it has a high collision efficiency for cloud droplets. The technique is relatively simple, low cost, requires low power (battery) and is suitable for use in primitive field conditions. The measurement is a new application of an older, commercially available aerosol particle sampling device which was originally designed for impaction sampling of fluorescent particles for airflow and dispersion measurements. In the present use, supercooled droplets rime onto a rapidly moving sampling wire, and the accumulated rime is removed and later weighed. This LWC measurement technique has been used routinely at the Elk Mountain Observatory (EMO), a research facility operated by the University of Wyoming, Department of Atmospheric Science. The purpose of this paper is to describe the operating characteristics of the device as applied to LWC measurement, to present calibration data and analysis and to compare simultaneous measurements of LWC from this device and two other instruments.

2. Description of the apparatus

The Rotorod (registered trademark of Metronics, Inc., Palo Alto, CA) consists of a small, constant rpm, direct current motor which rotates an H-shaped stainless steel flat wire (see Fig. 1). Airborne particles impact onto the leading edge of the wire; collection efficiencies for Zn–CdS aerosol particles are estimated by the manufacturer to be in excess of 60% for particles larger than 3 μm diameter (Leighton *et al.*, 1965). For calm conditions, the instantaneous geometric volume sampling rate of the leading edge of the wire is simply

$$d(\text{volume})/dt = 2\pi RFLY, \qquad (1)$$

where R is the radius arm (6 cm), F is the rotation rate (2350 rpm), L is the length of the leading edge (12 cm), and Y is the width of the wire perpendicular

[1] Present affiliation National Center for Atmospheric Research, Boulder, CO 80307.

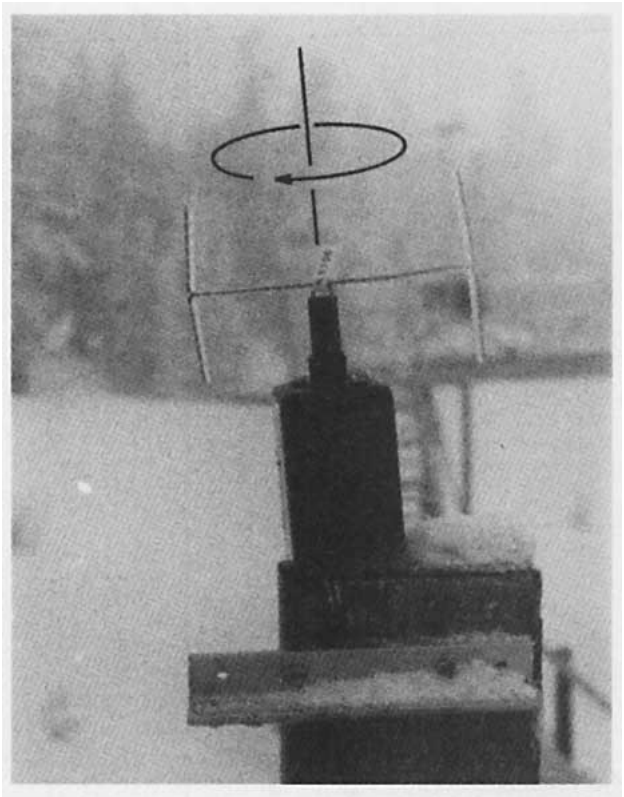

FIG. 1. Photograph of rimed Rotorod device. For size reference, the motor housing is 6 cm high. Rotation is about the vertical axis of the motor. Rime mass on the vertical arms of the wire and time of operation are used to calculate LWC.

to the relative airflow (0.042 cm). Stroboscopic measurements of F for four different motors and sampling arms indicated that F varied by less than 2% among the various units and that for any one motor, F was constant (±0.2%) for voltages in the range 9–14 V. Also, F was not affected by the addition of typical rime loads.

In its original use as part of tracer or dispersion studies, the wire is covered with a sticky black coating which collects airborne fluorescent particles for later microscopic counting or fluorometric analysis. The advantages of the device for field operation are that it is inexpensive, simple in design and operation, has low weight and requires small amounts of direct current power, as from a storage battery. Its chief disadvantage for aerosol sampling is the low collection efficiency which is sharply dependent on size for particles smaller than ~3 μm diameter.

We use this rotating wire device to collect rime ice during supercooled cap cloud conditions. The device is placed in an unobstructed part of the cloud and is switched on for periods of 5–30 min. Rime ice accumulates on the leading edge of the rime surface at a rate determined by the LWC of the cloud and the width of the collector. The previously mentioned disadvantage of collection efficiency for aerosol particles is not so serious for cloud droplets in our clouds, since most of the water mass (99%) is typically in the droplets larger than 6 μm diameter. The results of Ranz and Wong (1952) were used to estimate the collision efficiency for typical Elk Mountain cloud conditions. These computations indicated that the bare wire collides with droplets with a 50% efficiency at 2 μm diameter and 92% at 3.5 μm. Fig. 2 shows an average Elk Mountain cloud droplet mass distribution by size and also shows the calculated Rotorod collision efficiency; the mass distribution was determined by a cloud droplet replication technique (Squires and Gillespie, 1952). As rime accumulates on the wire, the leading edge grows wider, the collision efficiency decreases, and the volume sample rate increases. If the rime grows as wide as 3 mm perpendicular to the relative airflow, the collision efficiency decreases to minimum values of 50% at 5 μm and 90% at 9 μm (cf., Fig. 2). Rime widths larger than 3 mm were not observed since the rime is subjected to large centrifugal forces and breaks off if too much accumulates. Fig. 2 indicates that the bare wire has no collision efficiency limitations for the mass distribution shown, and the effect of reduced collision efficiency of the rimed wire is not a serious problem. Whether bare or rimed, the efficiency is relatively insensitive to changes in the droplet size distribution above ~9 μm where most of the mass (85%) is found in these clouds. For this mass distribution, only 1% of the mass is present in the droplets smaller than 6 μm diameter, below which the collision efficiency of the rimed wire is less than 60%; with a 3 mm rime width, the calculations indicate that a total of 2.8% of the

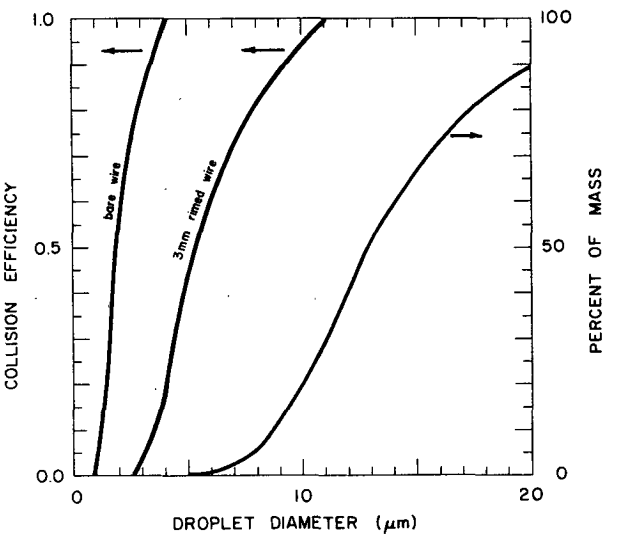

FIG. 2. Calculated droplet collision efficiency of the Rotorod wire, bare and rimed to 3 mm width, and an Elk Mountain cloud droplet mass distribution. The mass distribution was averaged from 89 size distribution measurements on 19 days in winter orographic clouds.

mass is not collected by the rimed wire. As shown later, this is approximately equivalent to the measurement uncertainty from instrumental and statistical errors.

The ambient wind has several effects on Rotorod sampling: it alters the collision efficiency of the wire; it alters the relative airflow past the wire, hence changing the shape of the rime deposit; and it increases the volume sampled. The collision efficiency of the wire is little affected by the wind speed, as long as the wind speed is substantially smaller than that of the collector arm (15 m s^{-1}). When the wind speed exceeds that of the collector arm, the collision efficiency increases. Leighton *et al.* (1965) estimated that for wind speeds of 22.5 m s^{-1}, this increase is ~10% and for 30 m s^{-1}, ~22%. The increase in sample volume was estimated by integrating the airflow relative to the wire, as follows: the airflow relative to the wire is $\mathbf{U} - \mathbf{V}$, where $\mathbf{U}$ is the ambient vector wind and $\mathbf{V}$ is the instantaneous vector velocity of the wire ($2\pi FR$). The length of air swept out per revolution is

$$\text{length} = R \int_0^{2\pi} [1 + C^2 + 2C \cos\phi]^{1/2}\, d\phi, \quad (2)$$

where $C = |\mathbf{U}|/|\mathbf{V}|$ and ϕ is the angle of rotation of the wire relative to the direction of the wind. Note that for zero wind, the length is $2\pi R$ and for very large wind speed, the length is $2\pi R|\mathbf{U}|/|\mathbf{V}|$ or $|\mathbf{U}|\tau$ since $|\mathbf{V}| = 2\pi R/\tau$, where τ is the time for one revolution. The integral (2) was evaluated numerically by a six-point Gaussian quadrature. The increase in sample volume over calm conditions amounts to 1% in a 3 m s^{-1} wind and 10% in a 9 m s^{-1} wind. Wind speeds at EMO are continuously measured with a propeller anemometer and typically are 2–5 m s^{-1} with gusts to 10 m s^{-1}. These speeds are presumed to not seriously affect the Rotorod LWC measurements since the combined effects of wind speed (increasing collision efficiency and sample volume) and rime growth (decreasing collision efficiency) are somewhat self-compensating and are approximately the same size as the measurement uncertainty.

After collecting rime ice, the wire is removed from the motor and taken into the heated laboratory; the rime ice is slipped off the vertical arms of the wire and into a weighing dish when the rime just starts to melt on the wire interface. Very little water mass is lost in this manner, and the process is repeatable and easily learned. The net rime accumulation (typically 100 to 500 mg) is weighed to an accuracy of ±1 mg. The rate of rime mass accumulation, mass per unit time, is converted to cloud liquid water by an equation which is derived in the following section.

To summarize, the advantages of this device are:

1) The measurement is simple, direct, suitable for remote or primitive locations, and relatively inexpensive.

2) Collection efficiencies are high enough for our orographic clouds that corrections for droplet size distribution are not usually needed.

3) The technique works in calm or windy conditions (in calm, the rotating wire fans the cloud past itself).

The fundamental limitations of the device are:

1) There is an upper limit to the measurable LWC which is dependent on temperature; i.e., to maintain "dry growth" of the rime, the cloud must be supercooled by more than ~4°C for LWC greater than 1.0 g m^{-3}. This limit was calculated from the equation which defines the critical limits for wet versus dry hailstone growth (e.g., Pruppacher and Klett, 1978, p. 566) using the dimensions of the bare or rimed wire. This calculated limit is consistent with our practical experience using the Rotorod.

2) Time resolution can be no better than the time needed to accumulate a measurable quantity of rime (~1 min for LWC of 1.0 g m^{-3} and ~60 min for LWC of 0.01 g m^{-3}).

3) Rime mass and exposure time must be measured to ~1% accuracy to achieve ~3% accuracy in LWC. Accuracy in the time measurement is easily met. If accuracy in the mass measurement is less than the ± 1 mg used in this study, the accuracy in LWC is degraded.

4) Manual handling and data reduction are necessary.

3. Relating rime rate and liquid water content

a. Shape of the rime deposit

The rate at which cloudy air is sampled is dependent upon Y, the width of the rime surface (1), and this width increases as rime accumulates during the sampling period. Calibration data in the form of rime mass measurements and photographs of rime deposits were collected during 1975, 1976 and 1977. Photographs, such as Fig. 3, were taken of the collected rime for a large range of cloud conditions. They revealed that the cross sectional shape of the rime was quite similar to conical graupel with the average angle from the vertex to the widest part of the rime consistently falling in the relatively narrow range of 55 ±5°. The constancy of this shape is illustrated in Fig. 4 which shows the traced rime cross-sectional outlines of several different samples; the figure also suggests how growth occurs. Some variations in the shape and density of the rime are expected, due to differences in relative airflow, temperature and cloud droplet size distribution. Since the maximum width of the rime is the important dimension needed to calculate the sample volume, it is useful to describe the cross-sectional shape mathematically. A theoretical derivation of the expected cross-sectional shape produced during

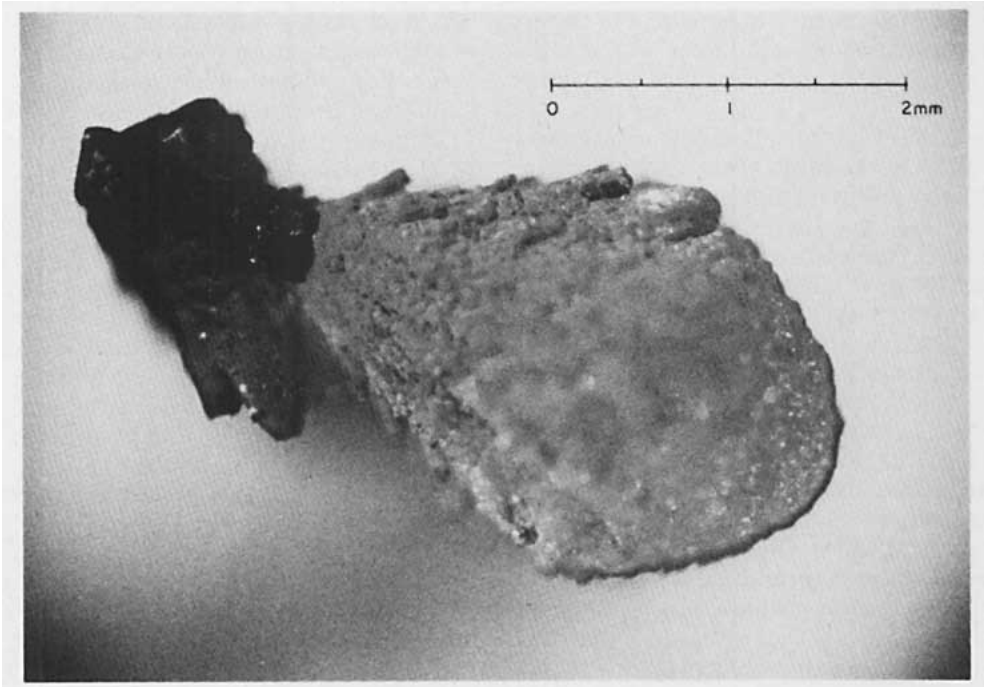

FIG. 3. Typical end view of rimed Rotorod wire; rime accumulates in a lemniscate shape on the upstream side of the wire.

rime growth would be quite involved and is probably not necessary for the present purpose. Of several common geometric shapes, the most similar to the rime shape is a lemniscate, shown in Figs. 5 (cf., Figs. 3 and 4). The lemniscate is described in polar coordinates (r and θ) by

$$r^2 = A^2 \cos(M\theta), \tag{3}$$

where A is the length of the major axis and M is a constant. Equations giving the cross sectional area of the lemniscate and the rime area follow from (3):

$$\text{inscribed area} = A^2/M, \tag{4}$$

$$\text{rime area} = A^2/M - D, \tag{5}$$

where D is the area of the wire.

The 65 rime photographs were analyzed for rime length $A - B$ on Fig. 5, and for the cross-sectional rime area by planimeter measurement. These data were then used to calculate, by a least-squares technique, the best value for M to obtain agreement between the calculated and measured lemniscate areas, as shown in Fig. 6. This resulted in a value for M of

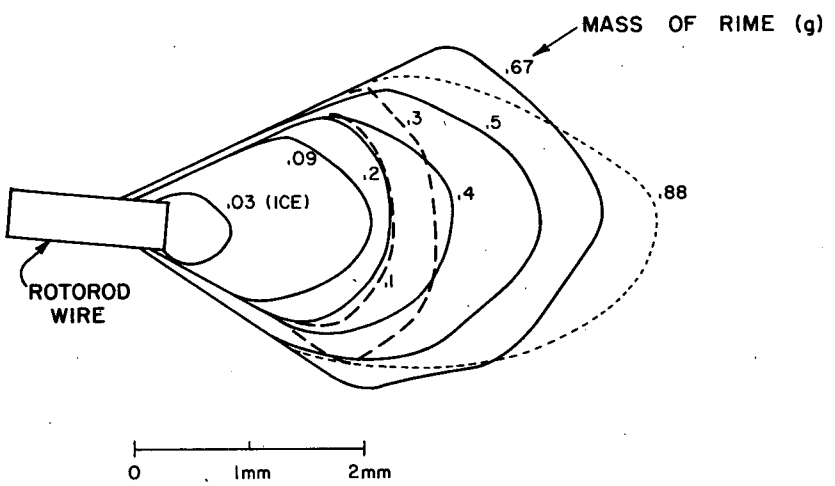

FIG. 4. Traces of rime deposits from several different photographic samples.

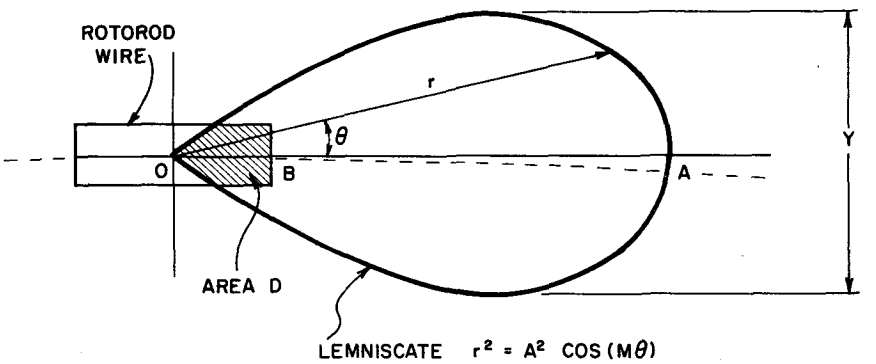

FIG. 5. Lemniscate curve with origin set into Rotorod wire. A and B are distances from origin along symmetry axis. Motion of the wire is also shown (dashed line).

2.60 ± 0.04 (probable error, including both measurement and statistical uncertainties). The value of M may depend upon cloud conditions (temperature, droplet sizes, etc.). The suggestion from Fig. 6 is that the lemniscate equation is a good approximation of the cross-sectional area and width of rime over the large range of values encountered. For a lemniscate, it can be shown that the maximum width of rime Y occurs at a half-angle θ, where $\tan(\theta)\tan(M\theta) = 2/M$; the solution of this equation for M of 2.6 is $\theta = 23°$, which is close to the measured half-angle from the photographs (27.5 ± 2.5°). For this lemniscate shape, the mathematically predicted maximum width is 0.56 × maximum length, that is, $Y = 0.56A$.

b. Approximate theoretical model

A first-order theoretical model was used to approximately describe the accumulation of rime on the wire. The lemniscate shape was assumed appropriate, and the shape factor M was assumed to be constant throughout the growth process. Given the following definitions (refer also to Fig. 5), χ is liquid water content, E is collision efficiency, A is maximum length of lemniscate, Y is maximum width of lemniscate, V is velocity of air relative to rime and m is mass of rime per unit length of wire; then, for geometrical scavenging of liquid water by the rime,

$$dm/dt = EYV\chi. \tag{6}$$

For the lemniscate shape,

$$m = A^2\rho_i/M \tag{7}$$

follows from (4), where ρ_i is the mass density of rime ice (assumed constant). For a fixed value of M, $Y = \alpha A$ and so

$$m = Y^2\rho_i/\alpha^2 M, \tag{8}$$

or

$$Y = \alpha[M/\rho_i]^{1/2}m^{1/2}. \tag{9}$$

Substitution of (9) into (6) yields

$$m^{-1/2}dm/dt = \alpha E[M/\rho_i]^{1/2}V\chi, \tag{10}$$

which was integrated and rearranged to obtain

$$\chi = \frac{2}{\alpha VE}\left[\frac{\rho_i}{M}\right]^{1/2}\frac{m^{1/2}}{t}, \tag{11}$$

or

$$\chi = \frac{2R}{LVEY_f}, \tag{12}$$

where R is the mass rime rate and Y_f is the final maximum width of the rime. Result (12) suggests that a measure of R alone is not sufficient to infer χ. At this point, finishing the problem to arrive at a numerical result becomes quite difficult because the rime density depends upon the droplet size distribution and the temperature and may vary within the

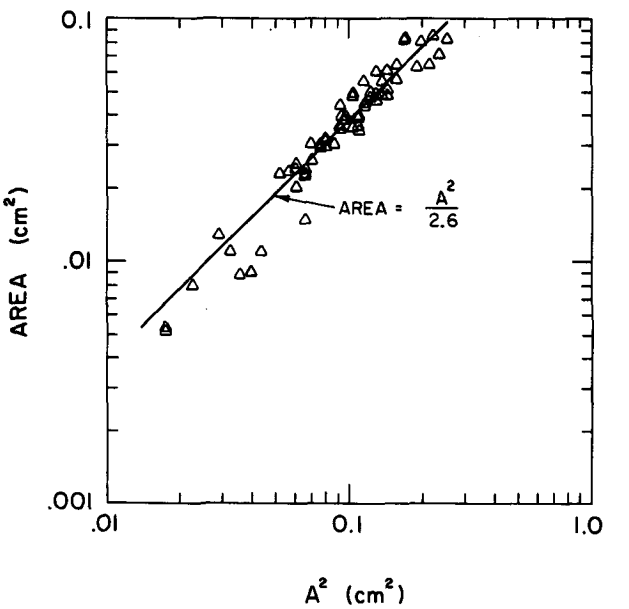

FIG. 6. Scattergram comparing the square of the lemniscate length A and the corresponding inscribed area from 65 planimeter measurements of rime photographs; also shown are the least-squares equation and curve.

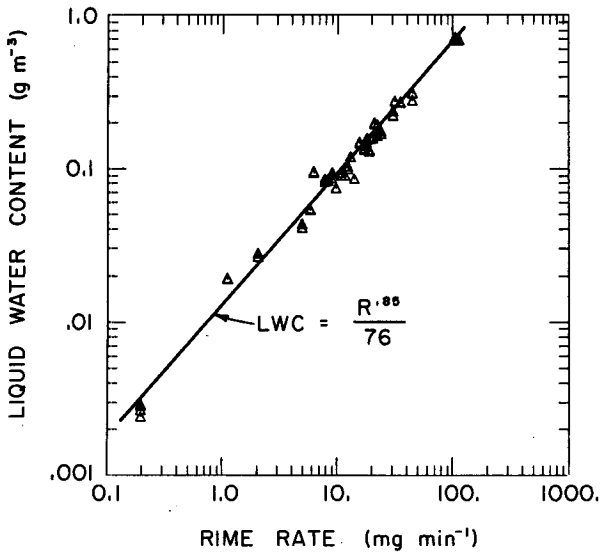

FIG. 7. Scattergram of measured Rotorod rime rate versus calculated LWC for 65 measurements; also shown are least-squares curve and equation.

rime deposit (Macklin, 1962). Furthermore, E is a function of the droplet size distribution, the ambient wind speed and Y_f. Y_f is itself dependent upon R and time and is observed to vary along the length of the wire. An empirical relation was investigated to see if it could provide closure to the problem, i.e., to uniquely relate R and χ.

Taking the derivative of (7) and equating it with (6),

$$2\frac{\rho_i}{M}A\frac{dA}{dt} = EYV\chi, \tag{13}$$

or

$$\frac{dA}{dt} = \frac{\alpha M}{2\rho_i}V\chi, \tag{14}$$

using $Y = \alpha A$. In a steady cloud, the rhs of (14) is constant, and so the depth of accumulated rime is directly proportional to time ($A - B = kt$). The mean value of the width of the collecting surface over a sampling period of duration T is

$$\begin{aligned} Y &= 1/T \int_0^T (Y_{\text{wire}} + 0.56kt)dt \\ &= Y_{\text{wire}} + 0.56kT/2 \\ &= Y_{\text{wire}} + 0.56[(M \times \text{inscribed area})^{1/2} - B]/2, \end{aligned} \tag{15}$$

using (4). Values for the area and B were determined from the photographic measurements. Because Y is increasing with time, the sampling rate (1) increases with time. In order to determine the relationship between rime rate and LWC, a plot and least-squares curve was constructed from the measured mass rime rates and the LWC. LWC was calculated from the mass and photographic measurements as

$$\text{LWC} = \frac{\text{measured mass}}{\text{mean volume sampling rate} \times \text{time}}, \tag{16}$$

where the mean volume sampling rate was obtained from (15) substituted into (1) for Y. The results of this comparison are shown in Fig. 7 for these data; also shown are the empirical least-squares equation and curve

$$\text{LWC} = (\text{mass/time})^{0.85}/76, \tag{17}$$

for mass in milligrams, time in minutes and LWC in g m^{-3}. Statistical uncertainties (probable error) associated with the exponent and denominator are ±0.0080 and ±2.1, respectively. The range of temperatures in these data was from −2°C (where rime resembled clear ice) to −17°C, and the range of measured rime densities was from 0.89 to 0.56 g cm^{-3}. The relation between mass rime rate and LWC is not expected to be linear since the volume sampling rate (1) is dependent upon the amount of accumulated rime. The correlation between rime rate and LWC is quite good, with linear correlation coefficients of +0.99 and, for the logarithms of the data, +0.99. The excellent correlation and small variance in the empirical relationship (17) suggest that for these clouds there are some compensating factors between the intractable parameters such that independent measurements of ρ_i in (11) or Y_f in (12) are not needed. This fortuitous result provides closure to the problem.

In the present results, there was no apparent dependency of rime density upon temperature (linear correlation coefficient 0.005), although one was expected according to the supercooled wind tunnel work of Macklin (1962). It is not clear that the present results conflict with Macklin's, since we did not measure the surface temperature of the rime (one of Macklin's parameters), and the scatter in our rime density values was too large to easily resolve a temperature trend. In Macklin's work a single parameter (temperature, impact speed or droplet size) was varied independent of the others; a similar situation probably did not occur in the natural orographic clouds of this study.

Frost growth and accretion of ice crystals to the riming surface probably occur and tend to exaggerate the LWC measurement. We have operated the Rotorod during snowfall when no significant liquid water cloud existed and found that no measurable amounts of ice were collected by the wire. Although the presence of the water cloud may enhance the frost and ice crystal accretion on the wire, this is not thought to pose a serious problem for our application since the mass flux of frost growth is small compared to the riming rate, and the ice content in these winter orographic clouds is normally a small fraction of the

TABLE 1. Instrument parameters.

Instrument	Sample volume	Sample time
Rotorod	0.5–3.0 m^3	5–30 min
Cloud gun	10 cm^3	5 ms
ASSP	10 cm^3	Continuous, recorded at 1 s intervals

liquid content. The extent of the problem for other environments has not been examined.

4. Comparisons with other instruments

The Rotorod has been routinely used for LWC measurements at EMO over the five-year period, 1974–80. During this time, a variety of other instruments has also been used for measuring liquid water as well as cloud droplet size spectra and concentration. In this paper, the two instruments whose liquid water measurements are compared to those of the Rotorod are the "cloud gun" and the Axially Scattering Spectrometer Probe (ASSP). The cloud gun is a replicating device which uses the impaction of water droplets on a soot-coated slide for the determination of droplet size and concentration (Squires and Gillespie, 1952). The measured size distribution is used to determine the liquid water content of the cloud; the mass distribution in Fig. 2 was derived from cloud gun measurements. The ASSP is an instrument manufactured by Particle Measuring Systems, Inc. (Boulder, CO), which sizes water droplets with diameters ranging from 2 to 45 μm by measuring the amount of light scattered by individual droplets. In addition to the differences in physical principles of operation, the three instruments to be compared differ greatly in their sampling volumes and times, as shown in Table 1.

The Rotorod was located 2 m above the roof of the corner of the observatory, or 8 m AGL. The ASSP was mounted in an inclined wind tunnel (26 m s^{-1} air speed), while the cloud gun samples were taken on the elevated platform which supports the upper end of the wind tunnel (5 m AGL). Fig. 8 shows the location of each of these instruments.

Four days in 1979 (January 9, 10, 16 and 18) were chosen for the intercomparison between the Rotorod and the other two instruments because of the large amount of data taken with each of the instruments and the wide range of cloud conditions. Within this data set, the droplet populations had concentrations ranging from 100 to 500 cm^{-3} with mean diameters of $\sim$10 μm. Liquid water contents ranged from 0.05 to as high as 0.5 g m^{-3}, and temperatures ranged from -8 to -13°C. These values are typical of wintertime orographic clouds in this region.

Fig. 9 shows the time trend measurement of liquid water by the ASSP, Rotorod and cloud gun over a period of four hours on one of the comparison days. During the observation period shown, the cloud temperature ranged from -12.8 to -13.2°C, and wind speed was from 3 to 5 m s^{-1}. This figure demonstrates the typical amount of variability of liquid water and the relative abilities of the instruments to indicate changes in liquid water. The ASSP values shown here were averaged over 60 s intervals. The figure indicates

FIG. 8. Photograph of the Elk Mountain Observatory showing the relative locations of ASSP, cloud gun and Rotorod.

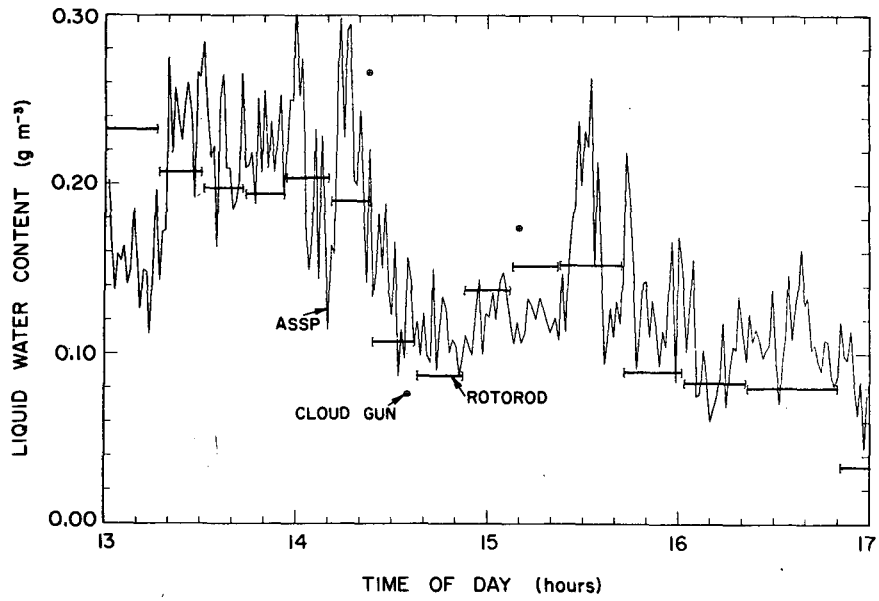

FIG. 9. Time trend of liquid water content measurements by the ASSP, Rotorod and cloud gun on 10 January 1979.

that the LWC was relatively uniform (variation generally within a factor of two) over the four hour period of sampling, and that temporal trends exist from time scales of the order of the full experimental period to less than the one minute averaging period of the ASSP. The amount of variation in the cloud liquid water is suggested by the fact that the standard deviation of the one second ASSP LWC measurements was ~43% of the mean value taken over an entire Rotorod time interval, and also by the variation in cloud gun values, which are typically of 5 ms duration. The Rotorod-measured LWC seems to track the temporal trends well for time periods of the order of or longer than its sampling period (~10 min). Since the Rotorod sampling rate increases with time, the average LWC values are weighted toward the end of their sampling periods. It is possible to gather shorter term Rotorod samples in order to better resolve temporal changes in liquid water. The lower limit to the sampling time for the Rotorod is a function of several variables: the skill of the operator and his speed in changing sampling wires is usually approximately one minute; the liquid water content and the resolution of the analytical balance also place restrictions on sampling times. In large LWC conditions, sampling times may be minimized, while small LWC values require longer sampling periods to accumulate sufficient rime mass.

Comparisons between simultaneous Rotorod LWC and ASSP LWC are shown in Fig. 10 for the four day data set containing 43 independent (no overlap) Rotorod sampling periods. For this comparison of Rotorod and ASSP data, the ASSP values were averaged over the intervals sampled by the Rotorod. A Rotorod and cloud gun comparison for 33 sampling intervals is shown in Fig. 11; several cloud gun slides were sometimes taken during one Rotorod interval. In both comparisons, the independent measurements of LWC are highly correlated with the corresponding Rotorod measurements (linear correlation coefficients of 0.94 and 0.73, respectively, for the ASSP and cloud gun), and the best fit lines have values close to the ideal 1.0 (0.98 and 0.79, respectively). A greater

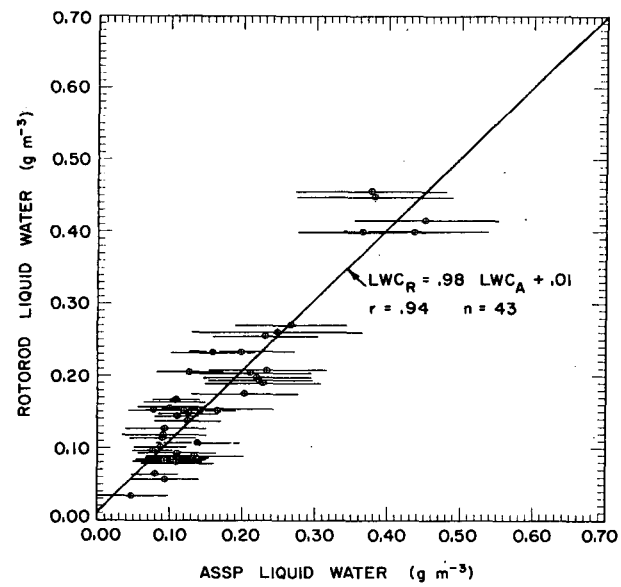

FIG. 10. Scattergram of Rotorod LWC versus ASSP LWC. Each point is a Rotorod measurement; 1 s ASSP values were averaged over each Rotorod sampling period. Horizontal bars show one standard deviation either side of the mean ASSP values.

amount of scatter is evident in the cloud gun–Rotorod comparison than the ASSP–Rotorod comparison. The majority of this scatter is probably attributable to the natural variation in cloud LWC over the five orders of magnitude difference in sampling times (or volumes) between the cloud gun and the Rotorod (cf., Table 1). Even with this variability there is still good agreement between the two instruments, lending support to the assumption of relative temporal stability of the cloud.

The last comparison was to plot the measured Rotorod riming rate against the averaged ASSP liquid water content for 43 sampling intervals. Fig. 12 shows the remarkably good agreement between the least-squares fit to these data and the empirical fit (17), using the method described in Section 3 and shown in Fig. 7. The close agreement between the ASSP independent measure of LWC and the Rotorod riming rate reinforces the assumptions used in deriving the sampling rate of the Rotorod. Also, if these ASSP data were used for an independent empirical calibration of the Rotorod, results nearly identical to the original work (Section 3) would be obtained.

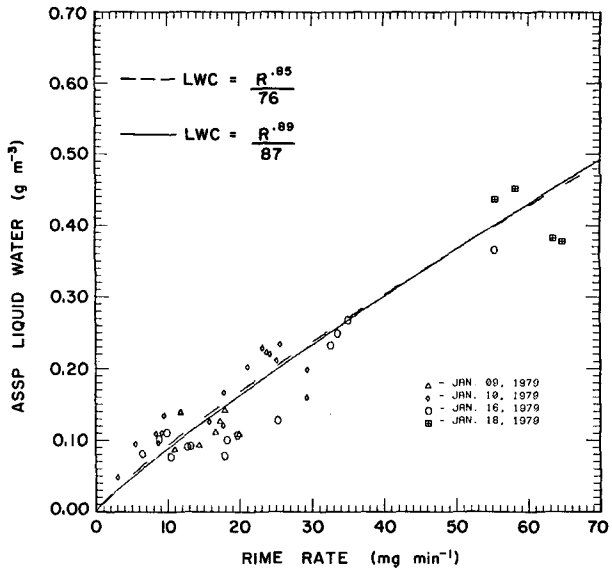

FIG. 12. Scattergram of measured Rotorod mass rime rate versus averaged LWC measured simultaneously by the ASSP. Solid line shows least-squares equation, and dashed line shows independently derived equation for comparison.

5. Conclusions

An inexpensive, portable, easy to operate device has been described for the measurement of supercooled liquid water content within a limited but useful range of temperatures, droplet diameters and LWC. Uncertainty of the LWC estimate depends upon the precision of the mass and exposure time measurements as well as the cloud conditions (wind, droplet size distribution, precipitation; etc.); the evidence presented here suggests an uncertainty of less than 5% for our application. Results from EMO for other cloud conditions support those presented in detail here. Additional characterizing work may be required if the technique is used outside the normal range of our cloud conditions: temperature colder than −4°C, LWC between 0.01 and 1.0 g m^{-3}, wind speeds less than 10 m s^{-1}, similar droplet size distributions, sample times sufficient to collect 0.1 to 0.5 g of rime ice, and no significant precipitation.

Using an empirical exponential relationship relating the rime accretion rate to LWC, the Rotorod demonstrates close agreement with other liquid water measuring instruments of greater cost and complexity. The technique serves as a useful reference measurement of LWC since mass is measured directly and not inferred, for example, from light scattering off of individual droplets (ASSP) or path length average light attenuation measurements. This device shows promise of being a practical instrument for use in supercooled environments with quasi-steady cloud conditions where the use of more complex instruments would be impractical.

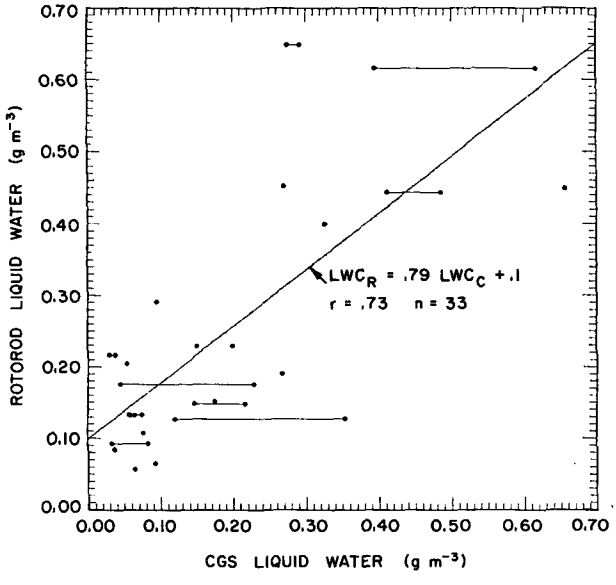

FIG. 11. Scattergram of Rotorod LWC versus cloud gun LWC. Connecting bars denote cloud gun samples taken during the same Rotorod sampling interval.

Acknowledgments. This research was sponsored by the Meteorology program, Atmospheric Science Section, National Science Foundation Grant ATM77-17540. The financial support of the NSF and the technical support of the Department of Atmospheric Science, University of Wyoming, are gratefully acknowledged.

REFERENCES

Brun, R. J., W. Lewis, P. J. Perkins and J. S. Serafini, 1955: Impingement of cloud droplets on a cylinder and procedure for measuring liquid-water content and droplet sizes in supercooled clouds by rotating multicylinder method. NACA Tech. Note 1215, 43 pp.

Chylek, P., 1978: Extinction and liquid water content of fogs and clouds. *J. Atmos. Sci.*, **35**, 296–300.

Dytch, H. E., and N. J. Carrera, 1976: Cloud droplet spectrometry by means of light-scattering techniques. *Atmos. Tech.*, **8**, 10–16. (Unpublished manuscript.)

Hill, G. E., and D. S. Woffinden, 1980: A balloonborne instrument for the measurement of vertical profiles of supercooled liquid water concentration. *J. Appl. Meteor.*, **19**, 1285–1292.

King, W. D., D. A. Parkin and R. J. Handsworth, 1978: A hot-wire device having fully calculable response characteristics. *J. Appl. Meteor.*, **17**, 1809–1813.

Kyle, T. G., 1975: The measurement of water content by an evaporator. *J. Appl. Meteor.*, **14**, 327–332.

Leighton, P. A., W. A. Perkins, S. W. Grinnell and F. X. Webster, 1965: The fluorescent particle atmospheric tracer. *J. Appl. Meteor.*, **4**, 334–348.

Macklin, W. C., 1962: The density and structure of ice formed by accretion. *Quart. J. Roy. Meteor. Soc.*, **88**, 30–50.

Pruppacher, H. R., and J. D. Klett, 1978: *Microphysics of Clouds and Precipitation*. D. Reidel, 714 pp.

Ranz, W. E., and J. B. Wong, 1952: Impaction of dust and smoke particles on surface and body collectors. *Ind. Eng. Chem.*, **44**, 1371–1381.

Squires, P., and G. A. Gillespie, 1952: A cloud droplet sampler for use on aircraft. *Quart. J. Roy. Meteor. Soc.*, **78**, 387–393.

Warner, J., and T. D. Newnham, 1952: A new method of measurement of cloud-water content. *Quart. J. Roy. Meteor. Soc.*, **78**, 46–55.